RAPID COMMUNICATIONS

PHYSICAL REVIEW B VOLUME 50, NUMBER 12 15 SEPTEMBER 1994-II

Intersubband L-valley and heavy-hole transitions in undoped GaSb/AlSb superlattices

Y. Abramovich, J. Poplawski, E. Ehrenfreund, and D. Gershoni
Department of Physics and Solid State Institute, Technion–Israel Institute of Technology, Haifa 32000, Israel

B. Brar and H. Kroemer
Department of Electrical and Computer Engineering, University of California, Santa Barbara, California 93106
(Received 29 April 1994; revised manuscript received 11 July 1994)

We report the observation of L-valley-conduction intersubband absorption concurrent with Γ-valence intersubband absorption in optically excited undoped binary-binary short-period GaSb/AlSb superlattices. Under above-band-gap optical excitation, electrons in these structures occupy the lowest-energy L-valley subband, while holes occupy the highest-energy Γ subband. Due to the separation in k space, these populations have long lifetimes, which enables the observation of photoinduced intersubband absorption. Due to the symmetry of the L valleys, their contribution to the intersubband absorption is observed for both s- and p-polarized infrared light, in agreement with theoretical predictions.

GaSb is known to have a small energy difference between the conduction-band minima at the Γ and L points ($E_L - E_\Gamma \simeq 90$ meV) and a large difference between the effective masses of electrons in these minima ($m_L/m_\Gamma \simeq 4$). Consequently, the quantum size effect can induce k-space direct-to-indirect transitions in a GaSb quantum well (QW).[1,2] As the GaSb QW size is reduced below $\simeq 4$ nm, the L subband becomes the lowest-energy conduction subband and the QW is said to have an indirect band structure. Photogenerated carriers in such narrow QW's have a long lifetime, typical for indirect band-gap semiconductors ($\simeq 0.1$ μsec).[3] Thus, even under continuous low-intensity interband pumping, considerable occupation of the lowest subbands can be built up.

Optically induced intersubband absorption was reported for QW structures in various material systems. Most of these studies were limited to direct semiconductors for which, under interband excitation and steady-state conditions, electrons occupy the lowest subband of the Γ valley.[4,5] In such structures, the intrinsic lifetime of the photogenerated carriers is relatively short (on the scale of nanoseconds), the steady-state population is small, and, hence, the observed induced absorption is small.[4] In cases where the photoexcited carriers are trapped (for instance, by potential fluctuations, impurities, or dislocations) their lifetime is considerably longer (a few μsec), and they contribute significantly to the observed induced absorption.[5,6]

In this paper we present a study of photoinduced absorption (PIA) in the GaSb/AlSb material system, in the indirect band-gap regime. We show that in the indirect band-gap superlattice (SL), both heavy-hole and L-valley electron intersubband absorption are induced by the above-band-gap radiation. We find that the confined-to-confined Γ heavy-hole absorption is polarized along the SL axis, whereas the confined-to-continuum transitions are polarized parallel to the SL interfaces. This is in agreement with a multiband effective-mass model. The confined-to-confined intersubband absorption due to the (111)-oriented L valleys is observed in both polarizations; similar to a recent study done on n-doped GaSb/AlSb SL's (Ref. 7) it is observed for light propagating along the (001) direction, which is normal to the SL faces. The observed ratio between the intensities of the two polarizations is in agreement with a simple single-band model.[8]

Three GaSb/AlSb samples were studied. They were grown by molecular-beam epitaxy on undoped, (001)-oriented GaAs substrates. The SL's which consisted of $\simeq 100$ periods of nominally undoped GaSb/AlSb layers, were grown on an AlSb buffer layer ($\simeq 0.5$ μm thick). Each period consisted of a GaSb QW layer of size d ($=2.5$, 3.5, or 4.5 nm) and an AlSb barrier layer of thickness b ($=7.5$, 6.5, or 6.5 nm), for samples I, II, or III, respectively.

To allow intersubband absorption measurements in both s- and p-polarization configurations, the samples were prepared as a multipass waveguide by polishing two parallel cleavage facets at a 45° angle [see inset in Fig. 1(a)]. The samples' dimensions were such that the IR beam traversed the SL $\simeq 10$ times in the area exposed to the pump beam.

All measurements were done using a Bruker IFS66V Fourier transform infrared spectrometer equipped with a step scan mirror movement to allow pump beam modulation in the frequency range of 100 Hz to 1 MHz using conventional lock-in techniques. We have used either the 514.5-nm Ar^+ line or a dye laser for the pump beam and an incandescent Nernst glower for the probe beam. In each polarization, both the transmission T and the photoinduced changes ΔT were measured, and the results are presented as $-\Delta T/T$. As sketched in the inset of Fig. 1(a), in the s-polarization geometry, the electric (E) field of the infrared radiation (IR), which propagates along the waveguide, has no component along the SL growth direction (z axis). In the p-polarization geometry, the IR E field is equally divided between the z axis and the xy plane. Thus, in order to correctly obtain the absorption and PIA polarization selection rules, the use of the two geometries is required. The s-polarization geometry yields the absorption and the PIA of the intersubband transitions for IR radiation polarized in the QW planes. Using this information, one can deduce the absorption and the PIA absorption of IR radiation polarized along the SL symmetry axis from the measurements in the p-polarization geometry. When the dark transmission of the sample is isotropic (e.g.,

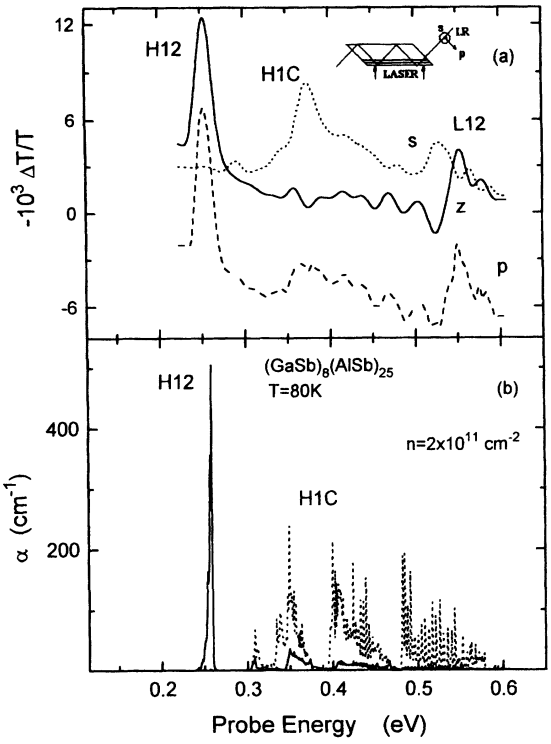

FIG. 1. (a) The PIA spectra $-\Delta T/T$ for sample I, excited with 1.65-eV radiation at 1 W/cm^2, taken at $T\simeq 80$ K. Dotted line, s polarization; dashed line, p polarization; solid line, z-axis polarization, extracted from the s- and p-polarization measurements using Eq. (1). The p-polarization curve is vertically displaced for clarity. Inset: the waveguide configuration and the definition of the directions of the s and p polarizations. In the s (p) polarization, the E field is perpendicular (parallel) to the plane defined by the growth direction and the IR beam direction. (b) Calculated intersubband absorption coefficient α for the geometry of sample I, assuming a hole density of $n=2\times 10^{11}$ cm^{-2}. The solid (dotted) line is for radiation polarized parallel (perpendicular) to the SL axis.

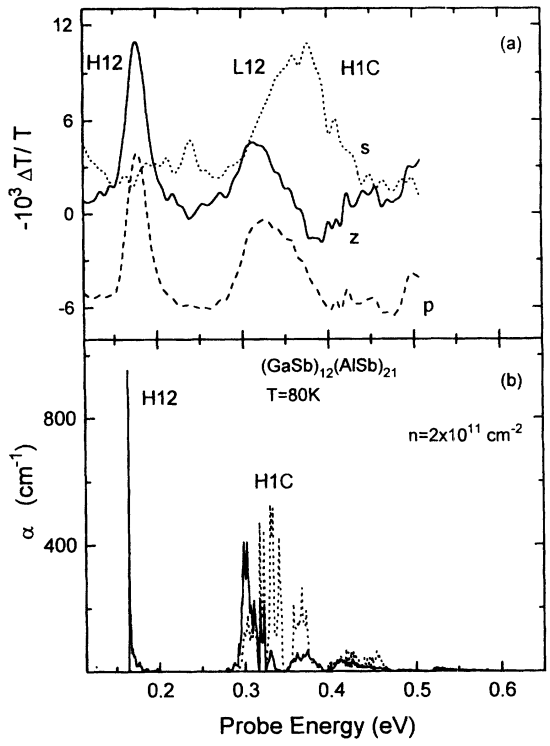

FIG. 2. Same as Fig. 1, but for sample II.

for undoped QW's) half of the measured $[-\Delta T/T]_p$ is due to the z-axis contribution and half due to the xy-plane PIA, in our 45° waveguide configuration. In this case, the net PIA along the growth direction is given by

$$\left[-\frac{\Delta T}{T}\right]_z = 2\left[-\frac{\Delta T}{T}\right]_p - \left[-\frac{\Delta T}{T}\right]_s . \tag{1}$$

Figure 1(a) displays the PIA measurements of sample I for the s and p polarizations in the energy range 0.1–0.6 eV. In the in-plane polarization (s geometry, dotted line), two bands are apparent. We denote the lower-energy band, which peaks at 0.37 eV, by $H1C$ (heavy hole 1 to continuum) and the higher one, which peaks at 0.55 eV, by $L12$ (L electron 1 to L 2). In the p-polarization geometry (dashed line) there appears an additional band (denoted $H12$, heavy hole 1 to heavy hole 2) centered around 0.26 eV. The net z-polarization PIA, $[-\Delta T/T]_z$, is obtained utilizing Eq. (1) and is plotted in Fig. 1(a) as a solid line. Comparing now $[-\Delta T/T]_z$ to $[-\Delta T/T]_s$ ($\equiv[-\Delta T/T]_{xy}$) we see that band $H12$ is polarized along the growth direction (z axis), the $H1C$ band is polarized in the xy plane, and the $L12$ band is observed in both polarizations.

Similarly, in Fig. 2(a) we display the PIA measurements of sample II. Here, since the GaSb QW's are wider, all the observed transitions are shifted towards lower energies. Band $H12$ appears at 0.186 eV, band $H1C$ at 0.36 eV, and band $L12$ at 0.32 eV.

We did not observe any PIA signal in sample III, where the GaSb QW's are 4.5 nm wide, which is above the indirect-direct crossover thickness (4 nm).[2] Thus, the photoexcited carrier lifetime in this direct SL sample is orders of magnitude shorter than the lifetimes of the indirect samples I and II. Consequently, the steady-state population of photoexcited carriers in sample III is too small to generate PIA signal which is large enough to be detected by our experimental technique. The lifetime of the photoexcited population, which gives rise to the PIA in samples I and II, was estimated from the PIA intensity dependence on the pump modulation frequency.[6] For sample II the estimated lifetimes are around 5 μsec, for all the bands observed. These long lifetimes are a few orders of magnitude longer than lifetime that was measured in a comparable undoped direct band-gap SL.[6] It shows that photoexcited carriers responsible for the observed PIA in these indirect SL's are intrinsically very long lived. We use these estimated lifetimes to get an estimation for the areal density of the steady-state population of photoexcited carriers. Typical values of 1×10^{11} cm^{-2} per well were deduced, in reasonable agreement with the calculated intensity of the PIA signal as discussed below.

We remark, though, that in both indirect and direct systems, extrinsic centers which trap the photoexcited carriers and inhibit their recombination, contribute significantly to the PIA signal. They reveal themselves in a typical sublin-

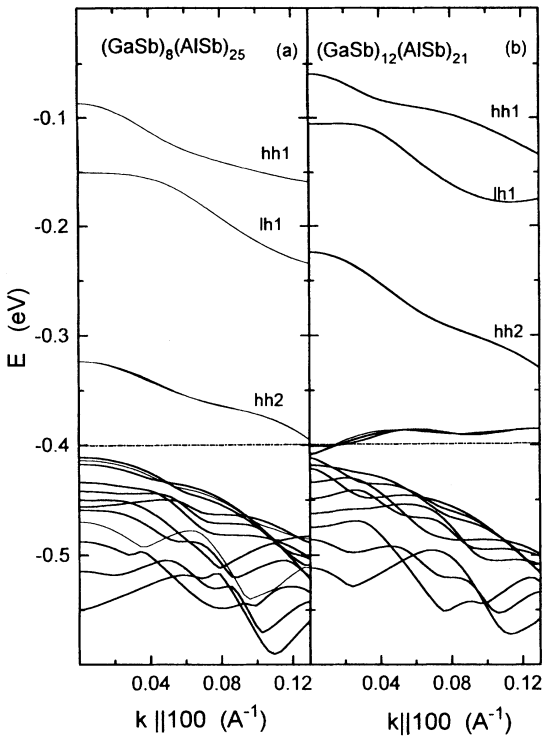

FIG. 3. Calculated SL valence-band dispersion relations for samples I (a) and II (b), plotted as energy vs in-plane wave vector, $k\|100$. The energy is measured from the top of the GaSb (well) valence band, and the dashed horizontal line at -0.4 eV marks the top of the barrier AlSb valence band.

earity and saturation of the PIA signal as the exciting pump intensity is increased.[6,9]

The identification of the various intersubband transitions observed, requires calculations which take into account both valence and conduction subbands. For a direct band-gap SL such a model was recently introduced by Gershoni, Henry, and Baraff (GHB).[13] Their model, which utilizes spatial plane-wave Fourier expansion of an 8×8 $\mathbf{k}\cdot\mathbf{p}$ effective Hamiltonian,[10] is valid only in the vicinity of the Γ point of the first Brillouin zones (BZ).[10] Currently, to the best of our knowledge, there is no theoretical model which incorporates, in a similar way, electronic subbands belonging to two different symmetry points within the BZ. We have thus chosen to calculate the valence intersubband transitions using the GHB model and to treat the conduction intersubband transitions in the indirect band-gap SL by a simple one-band Hamiltonian.[8]

The valence subband structure, calculated using the material parameters and deformation potentials of the binary compounds GaSb and AlSb,[11] are displayed in Figs. 3(a) and 3(b) for the geometries of samples I and II, respectively. The energies of the Γ valence subbands are plotted in the figures as a function of the in-plane crystal momentum $\mathbf{k}_\|$ along the (100) direction. For the calculations we have assumed that the GaSb layers are biaxially strained to match the lattice constant of the AlSb buffer layer. The low-lying confined energy levels are identified according to the number of nodes in their wave functions and their total angular-momentum projection on the superlattice symmetry axis at $\mathbf{k}_\|=0$. They are marked on the figure as either heavy holes ($M_J=\frac{3}{2}$, hh) or light holes ($M_J=\frac{1}{2}$, lh). In addition, there are minibands of extended states below the AlSb barrier valence-band energy. These valence continuum minibands are similar to the conduction continuum minibands which were observed recently above the barrier energy in direct band-gap SL's.[12] The matrix elements for optical transitions between the various states are calculated using the dipole approximation and the calculated wave functions.[13] In order to calculate the PIA, we have used the experimentally estimated steady-state hole density ($\simeq2\times10^{11}$ cm^{-2} per well) assuming thermal equilibrium. We then summed over all the allowed optical transitions from occupied to unoccupied states. The complex nature of the valence minibands in the continuum (Fig. 3), requires caution in the actual summation. We find that in order for the calculation to converge, a large number of points in the $\mathbf{k}_\|$ plane, as well as many Fourier components parallel to the SL axis, are required. For example, in order to obtain Figs. 1(b) and 2(b), which display the calculated valence intersubband absorption for samples I and II, we summed over more than 2000 points equally distributed in 50 different directions in the first 10% of the $\mathbf{k}_\|$ plane closest to the Γ point, and used 41 Fourier waves along the SL direction. The calculated intersubband absorption spectra are described by solid (dotted) lines for light polarized along the z axis (xy plane). We note that the various valence intersubband transitions are polarized very differently. The hh1 $\rightarrow$hh2 transition (marked $H12$) is polarized along the z axis, whereas the transitions hh1$\rightarrow$ continuum (marked $H1C$) are polarized almost entirely in the xy plane. Likewise, the hh1 $\rightarrow$lh1 absorption (at $\simeq65$ meV for sample I and $\simeq52$ meV for sample II, not shown) is also polarized in the xy plane. Comparing the spectral position and polarization of band $H12$ observed by PIA, for sample I, to the calculated spectrum [Fig. 1(b)], we can clearly identify $H12$ (Fig. 1) as the hh1$\rightarrow$hh2 transition. The observed band $H1C$ [Fig. 1(a)] has the same polarization (xy) as the calculated one, and it spans an energy range which is approximately where the calculated hh1$\rightarrow$ continuum transitions appear. The xy polarization of these transitions is the result of the character of the continuum minibands (heavy or light holes). Their energy, on the other hand, is extremely sensitive to material constants, which are not very accurately known,[11] and the structural geometry. In our calculations we have used the nominal layer thickness, as estimated from the growth rate. Therefore, some differences in band shape and position are to be expected. We then conclude that the observed $H1C$ is due to hh1$\rightarrow$ continuum transitions, although their spectral shape differ as seen in Fig. 1. For sample II, the $H1C$ and $L12$ bands overlap in energy and a detailed comparison is more difficult even in the z polarization geometry, since both bands are not completely polarized. We then conclude that in the energy range marked by $L12$ and $H1C$ [Fig. 2(a)], we observe contributions from both $L1$ to $L2$ and from hh1 to the continuum.

The L-valley energy levels were calculated using the standard single-band envelope-function approximation. We have used band offset of $\Delta E_c(L)=1.0$ eV,[14] effective masses of $m_\Gamma^*=0.041m_e$ and $0.11m_e$ for GaSb and AlSb, respectively,[14,11] and $m_t=0.11m_e$, $m_l=0.95m_e$, yielding quantization mass[15] of $m_z^*=3m_lm_t/(2m_l+m_t)=0.16m_e$ for

TABLE I. The calculated L-valley energy levels, $L1$ and $L2$, the difference $L1-L2$, and the measured transition energies of band L (Figs. 1 and 2), for samples I and II.

	$\Gamma 1$ [a] (eV)	$L1$ (eV)	$L2$ (eV)	$L2-L1$ (calc.) (eV)	band L (expt.) (eV)
Sample I	0.28	0.22	.0.76	0.54	0.55
Sample II	0.14	0.12	0.45	0.33	0.32
Sample III	0.08	0.08	0.32	0.24	

[a]The values of $\Gamma 1$ are relative to the bottom of the L QW, which is assumed to be $\simeq$90 meV above the bottom of the Γ QW.

the L valley in both GaSb and AlSb. Strain and nonparabolicity were not included in the L-valley calculations. The energies obtained for the L-valley subbands for all samples are summarized in Table I, along with the experimental values observed in samples I and II for band $L12$.

In (001)-oriented GaSb QW's, intersubband absorption within the (111)-oriented ellipsoidal L valleys occurs both for light polarized parallel and perpendicular to the QW planes. In our 45° waveguide geometry, the squares of the IR vector potential components along the z axis and in the xy plane are, respectively, $A_z^2=A_p^2/2$ and $A_{xy}^2=A_p^2/2+A_s^2$, where A_s and A_p are the components along the s and p directions [see the inset in Fig. 1(a) for a description of these directions]. Using the calculations of Brown and Eglash,[8] the geometrical factors associated with the s and p polarizations are $G=[m_z^*(m_l-m_t)/3m_lm_t]^2$ and $(1+G)/2$, respectively. For GaSb, we find $G=0.2$, so a ratio of $[\Delta T/T]_p/[\Delta T/T]_s=(1+G)/2G\simeq 3$ is expected, in close agreement with the ratio of $\simeq 2$ found experimentally in sample I for band $L12$ [in sample II, band $L12$ overlaps $H1C$, see Fig. 2(a)]. Thus, based on the energy subband calculations (Table I) and the polarization, we assign band $L12$ to the $L1$ to $L2$ intersubband absorption. At this point we note that band $L12$ [Fig. 1(a)] appears to have slightly different energy ($\simeq$20 meV) for s and z polarizations. This difference may be the result of the removal of degeneracy between the xy and the z states of the L valley. Similar effect was observed for the X valley at short-period AlAs/GaAs superlattices.[16]

In summary, we have presented the observation of photoinduced absorption of indirect SL's, and identified both heavy-hole and L-valley intersubband transitions. Due to the indirect k-space band gap, the lifetimes of the photoexcited carriers are relatively long and consequently, large modulation ($>1\%$) of the relative transmission is obtained. The confined hh1-hh2 intersubband absorption was found to be polarized along the growth direction, while the hh1 to continuum miniband absorption was found to be polarized mostly in the plane perpendicular to the growth direction. The (111)-oriented L-valley contribution to the intersubband absorption is observed both for polarization along the (001) QW axis, or along the QW planes. Both the hh1 to continuum and $L1$-$L2$ transitions could thus be observed for normal incidence IR light.

The work at the Technion was carried out in the Center for Advanced Opto-Electronics, and was partly supported by the Vice President Fund for the Promotion of Research. The work at UCSB was supported in part by the Office of Naval Research, and in part by the Jet Propulsion Laboratory.

[1] G. Griffiths, K. Mohammed, S. Subbanna, H. Kroemer, and J. L. Merz, Appl. Phys. Lett. **43**, 1059 (1983).

[2] A. Forchel, U. Cebulla, G. Tränkle, H. Kroemer, S. Subbanna, and G. Griffiths, Surf. Sci. **174**, 143 (1986).

[3] U. Cebulla, A. Forchel, G. Tränkle, S. Subbanna, G. Griffiths, and H. Kroemer, Phys. Scr. **35**, 517 (1987).

[4] M. Olszakier, E. Ehrenfreund, E. Cohen, J. Bajaj, and G. J. Sullivan, Phys. Rev. Lett. **62**, 2997 (1989).

[5] J. Oiknine-Schlesinger, E. Ehrenfreund, D. Gershoni, D. Ritter, M. B. Panish, and R. A. Hamm, Appl. Phys. Lett. **59**, 970 (1991).

[6] Y. Garini, E. Ehrenfreund, E. Cohen, Arza Ron, K-K. Law, J. L. Merz, and A. C. Gossard, Phys. Rev. B **48**, 4456 (1993).

[7] L. A. Samoska, B. Brar, and H. Kroemer, Appl. Phys. Lett. **62**, 2539 (1993).

[8] E. R. Brown and S. J. Eglash, Phys. Rev. B **41**, 7559 (1990).

[9] E. Ehrenfreund, J. Oiknine-Schlesinger, D. Gershoni, D. Ritter, M. B. Panish, and R. A. Hamm, Surf. Sci. **267**, 461 (1992).

[10] G. A. Baraff and D. Gershoni, Phys. Rev. B **43**, 4011 (1991).

[11] *Semiconductors*, edited by O. Madelung, M. Schulz, and H. Weiss, Landolt-Börnstein, New Series, Group III, Vol. 17, Pt. a (Springer-Verlag, Berlin, 1982).

[12] D. Gershoni, J. Oiknine-Schlesinger, E. Ehrenfreund, D. Ritter, R. A. Hamm, and M. B. Panish, Phys. Rev. Lett. **71**, 2975 (1993).

[13] D. Gershoni, C. H. Henry, and G. A. Baraff, IEEE J. Quantum Electron. **29**, 2433 (1993).

[14] U. Cebulla, G. Tränkle, U. Ziem, A. Forchel, G. Griffiths, H. Kroemer, and S. Subbanna, Phys. Rev. B **37**, 6278 (1988).

[15] F. Stern and W. E. Howard, Phys. Rev. **163**, 816 (1967).

[16] E. Finkman, M. D. Sturge, and M. C. Tamargo, Appl. Phys. Lett. **49**, 1299 (1986).